Goodput Estimation for an Access Node Buffer Carrying Correlated Video Traffic

A. Awad M. W. McKinnon R. Sivakumar
ashraf@cnd.gatech.edu b.mckinnon@ieee.org siva@ece.gatech.edu
Georgia Tech Research Institute School of Electrical and Computer Engineering
Georgia Institute of Technology
Atlanta, GA 30332-0250

Abstract

In this work, we present an algorithm to analytically estimate the frame goodput of a correlated MPEG-2 video source that traverses a first network node's buffer; where frame goodput is defined as the ratio of the number cells in completely and correctly transmitted frames through the buffer to the total number of cells arriving to the buffer. The effect of changing the output-to-input line speeds on the frame goodput is also investigated. By using this algorithm, a buffer that is three times the maximum frame size is seen to yield loss probability of 10^{-6} *at a normalized output line rate of* 0.28 *for a load of* 20%*. A maximum simulation error margin of ± 30% for values in the order of* 10^{-5} *with a 98% confidence was achieved.*

1 Introduction

The fast growth in high-speed, multimedia communication networks has enlarged the spectrum of bandwidth consuming applications offered to the users. These applications have caught the interest of many research groups who focused on data compression, with their goal being to optimally utilize the bandwidth and resources that such applications require. Due to the effectiveness of video compression schemes such as MPEG-2 [8], it becomes important to understand VBR video traffic characteristics in order to efficiently allocate resources to these traffic flows. VBR video traffic behavior affects traffic flow at network buffers and switches, especially at network congestion when buffer overflow is a possibility; this congestion in turn, directly affects video quality of service (QoS). A typical type of network for accommodating multimedia applications is an ATM network, because it supports several levels of QoS, including VBR traffic [5, 3]. Data-Over-Cable networks that use DOCSIS[1] is another contemporary network for handling multiplexed multimedia applications.

Our work is concerned with cell[2] loss that is caused by overflow of the output link buffer at the network access node, specifically the overflow encountered at the first network hop on a flow's route. Due to the structure of an MPEG-2 stream, the impact of a lost (or corrupted) packet will not only result in the affected frame not being correctly displayable at the destination, but the impact of the error may "ripple" through other subsequent frames due to their dependence on the corrupted frame. The conventional cell loss ratio measurement does not capture the impact of these errors. However, by considering error propagation in cell loss calculations through goodput analysis, we expect to have a better estimate of video quality that will lead to better human perception measures discussed in [10]. Unfortunately, it is hard to accurately measure the error propagation loss because information within a frame has different significance. For example, system information, slice headers, and motion vectors are more important than other data in the frame. Layered coding [11], error concealment [3], and error resilience techniques have been proposed for reducing the effect of cell loss having the result of improving the stream's perceived quality.

In this study, we propose a method to estimate and measure the frame goodput at the first of a series of network node's buffer for a correlated MPEG-2 input source. We define the frame goodput as the ratio of the outgoing cells of good and correctly displayable frame to the total number of frame cells that arrive at the buffer. Hence, the goodput is a measure of the amount of the traffic that is transported without any errors. The cell discard process is specific for the structure of an MPEG-2 stream and it is guided by the dependencies between frames in determining what data to

[1] Data Over Cable Service Interface Specifications.

[2] We define a cell as the network transport packet for any general slotted system. It is not specific to ATM only.

discard. The estimation method's results are validated by simulation results. The system we use is generic and applies to most slotted communication systems. A single video traffic source is used in this work to present the accuracy of the estimation method for a simple case, which we will extend in subsequent work. In addition, we present primary performance results that can be extended in later work to study cases with multiplexed sources and priority cell discard, which involves more factors to account for. This single source case can also be considered as an approximation for a Weighted Fair Queueing (WFQ) scheduling technique in a multiplexed system with a fixed buffer allocation for each source.

The paper is organized as follows. In Section 2, we present previous work on cell loss improvement and over slotted networks. In Section 3, we give a background of MPEG-2 structure and standard, and describe the system that we are studying. In Section 4, we illustrate the proposed estimation method analysis. In Section 5, we describe the simulation process and present the results. Finally, we conclude our work in the Section 6.

2 Previous Work

There has been similar work on video estimation and goodput in literature. In [7], the authors studied goodput of MPEG CBR traffic. They developed a goodput control approach to drop frames based on buffer overflow, dependencies between frames, and frame transmission deadline. The results showed the improvements of goodput control through increasing the number of useful frames in the received packets. The goodput measurement was computed at the frame level, which is a reasonable estimate of goodput when frame sizes are equal. This frame level measurement would not be accurate if applied for VBR MPEG video as in our case due to difference in frame sizes between different frame types. Hence, we use smaller fixed size cells to measure goodput.

In [12], the authors used MPEG video traces to generate the MPEG video source model and then approximated the cell loss process by a two-state Markov chain (Gilbert model). They showed that, under the same network condition, long burst cell loss results has a better human perception than having multiple short cell loss bursts, which applies to the dropping scheme in goodput analysis. They defined the Mean Opinion Score as a subjective measure of each MPEG clip; and the smallest value of the moving average of the peak signal-to-noise ratio of each frame as a quantitative measure.

In [2], an algorithm for fair bandwidth sharing in the core network without per-flow state was presented. Each flow was divided into sets of layers and packets are marked at an edge router with layer label (color) according to flows bit rates. When congestion occurs, the core router discards packets with highest label number. That scheme was applied in evaluate to the goodput of video traffic. However, it only served as a priority scheme since, after congestion ends, the core router does not explicitly discard video frames that reference a previously dropped frame during the congestion.

Given the frame dependencies in an MPEG-2 video stream, frame goodput is a useful metric that can indicate the worst case perceived quality of a transmitted video stream. To our knowledge, there is no direct work that has been done on video traffic frame goodput measurement and estimation.

3 System Description and Abstraction

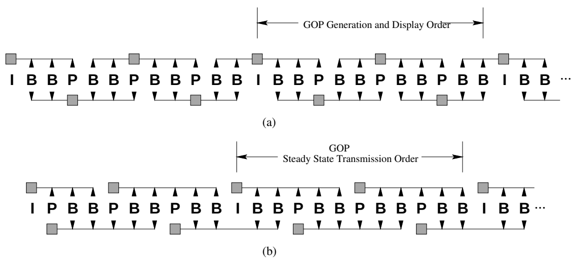

Figure 1. Dependencies between MPEG-2 frames in the transmission order.

In order to transmit a video stream in the system from the source to the first hop, frames are segmented into cell sizes according to the network protocol applied, and then transmitted. Figures 1(a) and (b) give the order and dependencies among frames during both frame generation and display, and during transmission, respectively. The frames are reordered prior to transmission so that frames are transmitted before all dependent frames. The reordering of frames creates an overlap between consecutive GOP boundaries, which makes goodput analysis more difficult.

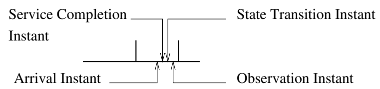

Figure 2. Pessimistic event order within a slot.

When the buffer overflows during a receipt of a frame, it drops ensuing cells that belong to that frame. Due to the information dependencies among the video frames, dependent frames cannot be fully reconstructed when they arrive their destination and are discarded[3]. Hence, when a

[3]Error concealment algorithms can be applied to corrupted frames and

$$\mathbf{P} = \begin{array}{c} \tau_{\downarrow}^{\rightarrow} \\ 0 \\ 1 \\ \vdots \\ \\ \\ TW-1 \end{array} \begin{array}{c} \begin{array}{cccccc} 0 & 1 & & & \cdots & TW-1 \end{array} \\ \begin{pmatrix} 0 & \mathbf{R}(0) & 0 & & \cdots & 0 \\ 0 & 0 & \mathbf{R}(1) & 0 & \cdots & 0 \\ \vdots & \vdots & & \ddots & & \vdots \\ & & & & & 0 \\ 0 & 0 & & & \cdots & \mathbf{R}(TW-2) \\ \mathbf{R}(TW-1) & 0 & & & \cdots & 0 \end{pmatrix} \end{array} \quad (1)$$

B-frame causes the buffer to overflow, only that B-frame is discarded. However, when an anchor frame causes the buffer to overflow, other frames in the GOP are also discarded. In our system, we will not empty the buffer of the arrived cells that belong to a discarded frame before the overflow happens; this is an approximation to the goodput in order to accommodate the definition of Tail Drop scheme and to simplify the theoretical analysis significantly. Emptying the buffer will also make it difficult to implement in practice. Buffered traffic is then served in a FIFO fashion by being transmitted over the output link to its destination.

4 Queueing Analysis

In order to analyze the system described in the previous section, a Markov chain was embedded at the observation instants at the end of each slot. In this study, we assume the order of simulation events is as shown in Figure 2. This queueing system is analyzed using a five dimensional Markov chain with a state representation (t, w, z, y, x), where:

- t is the slot number in a frame period of time, such that $t \in \{0, 1, 2, \cdots, T-1\}$;
- w is the frame number in a GOP, such that $w \in \{0, 1, 2, \cdots, W-1\}$[4];
- x indicates if the current frame has completely arrived or not, such that $x \in \{0, 1\}$;
- z indicates if the buffer is accepting cells, overflowing on their arrival, or not accepting them, $z \in \{accept, dropframe, dropGOP, dropGOP{*}\}$; and,
- y is the instantaneous length of the queue, such that $y \in \{0, 1, 2, \cdots, B\}$.

Given the state description above, we notice that the repeating structure of the GOP may be exploited to realize a p-cyclic Markov chain representing the transition probability between slots of a GOP. The state machine's probability transition matrix has the block form given in (1). **P** is a $TW \times TW$ p-cyclic block matrix that contains a top level description of the cyclic state machine mentioned earlier[5]. Each block matrix represents transition probability matrix between consecutive slots in the GOP. The dimension of the block matrix is equal to the total number of slots in the GOP whether they are occupied with cells or empty. We define the value τ, where $\tau = \tau(t, w) = wT + t$, to reference slots in the GOP when distinction between frame boundaries is not necessary.

$$\mathbf{R}(t, w) = \begin{array}{c} x_{\downarrow}^{\rightarrow} \\ 1 \\ 0 \end{array} \begin{array}{c} \begin{array}{cc} 1 & 0 \end{array} \\ \begin{pmatrix} \mathbf{C}_a & \mathbf{C}_n \\ 0 & \mathbf{C}_n \end{pmatrix} \end{array} \quad (2)$$

The submatrices $\mathbf{R}(t, w)$ describe the system behavior during the transition between the end of slot τ and the end of slot $\tau \oplus 1$ [6]. Cells arrive in bursts (frames) according to the video frame structure; these bursts arrive at a constant burst rate (25 or 30 frames per second). Cell bursts are usually followed by unused slots. We notice that in any slot, exactly one of two cases can occur: a cell arrival or no cell arrival at the buffer. We describe each case with a separate submatrix due to their different effects on the system behavior. These two matrices are used in defining $\mathbf{R}(t, w)$. The first matrix, denoted as $\mathbf{C}_a = \mathbf{C}(t, w, 1)$, represents the case of the system transitioning from a slot τ to slot $\tau \oplus 1$ given that an arrival occurs during slot $\tau \oplus 1$. Similarly, the second matrix, denoted as $\mathbf{C}_n = \mathbf{C}(t, w, 0)$, represents the case of the system transitioning from a slot τ to slot $\tau \oplus 1$ given that *n*o arrival occurs during slot $\tau \oplus 1$. Using these two matrices, we can write the general structure of $\mathbf{R}(t, w)$ in the form given in (2).

Consider the previously mentioned $\mathbf{C}(t, w, x)$ submatrices. In each submatrix, we can define four different states to describe the buffer's behavior; we will denote them as *accept, drop frame, drop GOP*, and *drop GOP**.

In the *accept* state, the buffer performs the normal operation of receiving and enqueueing cells, if adequate space

some information can be retrieved, however, their effect is not considered here in the goodput analysis.

[4]The frames in a GOP are numbered according to their transmission order, therefore, the B-frames numbered 1 and 2 correspond to the last two frames of the previous GOP.

[5]The total size of **P** is $8TWB \times 8TWB$, which reduces to $8B \times 8B$ when solved using LU decomposition.

[6]Note that the symbol $\oplus$ denotes modulo-(TW) addition.

$$
\mathbf{C} = \begin{array}{c} z_{\downarrow}^{\rightarrow} \\ accept \\ D'frame \\ D'GOP \\ D'GOP* \end{array}
\begin{array}{c}
\begin{array}{cccc} accept & D'GOP & D'frame & D'GOP* \end{array} \\
\begin{pmatrix}
\mathbf{D}_{11} & \mathbf{D}_{12} & \mathbf{D}_{13} & \mathbf{D}_{14} \\
\mathbf{D}_{21} & \mathbf{D}_{22} & \mathbf{D}_{23} & \mathbf{D}_{14} \\
\mathbf{D}_{31} & \mathbf{D}_{32} & \mathbf{D}_{33} & \mathbf{D}_{14} \\
\mathbf{D}_{41} & \mathbf{D}_{42} & \mathbf{D}_{43} & \mathbf{D}_{44}
\end{pmatrix}
\end{array} \tag{3}
$$

exists. When the buffer overflows, it starts discarding arriving cells. The length of cell discard depends on the frame type during which overflow occurs. If the buffer overflows while receiving a B-frame, the buffer state transitions to the *drop frame* state because the cells of that frame are the only cells to be discarded before it returns to the *accept* state. If the buffer overflows during receiving an anchor frame, however, the buffer transitions to the *drop GOP* state because cells of the rest of frames during the current GOP are to be discarded.

In the GOP transmission order, frames are rearranged according to inter-dependencies between frames. This rearrangement introduces an overlap in the boundaries between successive GOPs because the last two B-frames in a GOP are dependent on the I-frame of the next GOP, and that I-frame has to be transmitted before these B-frames. In the *drop GOP** state the buffer accepts the I-frame of the next GOP and drops the following two B-frames then transitions to *accept* state. In the *drop GOP* state, the buffer drops the frames until it transitions to *drop GOP** when it starts receiving a new I-frame. The difference between *drop GOP* and *drop GOP** is that, in the latter, the I-frame that belongs to the next GOP is skipped when dropping the current GOP while in the former the I-frame that belongs to the current GOP is dropped.

Each of the $\mathbf{C}(t, w, x)$ matrices has the general structure given in (3) (where *drop* is abbreviated as *D*). We will elaborate on the possible forms of $\mathbf{D}_{ij}(t, w, x, z)$ so tht the specific structure of $\mathbf{C}(t, w, x)$ will become clear.

The matrix $\mathbf{D}_{ij}(t, w, x, z)$ is a $(B + 1) \times (B + 1)$ matrix; it describes the instantaneous buffer length at each observation instant given the submatrix' position in **P**, which defines the y dimension in the Markov chain. We use three types of $\mathbf{D}_{ij}(t, w, x, z)$ matrices that are useful in defining the $\mathbf{C}(t, w, x)$ matrices; these matrices are $\mathbf{D}_f = \mathbf{D}(t, w, 1, 0)$, $\mathbf{D}_e = \mathbf{D}(t, w, x, 1)$, and $\mathbf{D}_t = \mathbf{D}(t, w, 1, 2)$[7]. The matrix $\mathbf{D}_f$ represents the buffer's operation under normal conditions when there are cell arrivals and no buffer overflow. $\mathbf{D}_f$ has the form given in (4), where α (in cells/slot) denotes the mean buffer service rate. Since there is a cell arrival, the buffer size either increases or remains constant depending on the occurrence of a cell departure.

$$
\mathbf{D}_f = \begin{bmatrix}
0 & 1 & 0 & \cdots & 0 \\
0 & \alpha & 1-\alpha & & \vdots \\
\vdots & & \ddots & \ddots & 0 \\
 & & & \alpha & 1-\alpha \\
0 & \cdots & & 0 & 0
\end{bmatrix} \tag{4}
$$

The matrix $\mathbf{D}_e$ describes the buffer's operation when it is not accepting cells either because the buffer is discarding arriving cells due an earlier overflow, or because there are no cell arrivals at all. Therefore, $\mathbf{D}_e$ has the form given in (5). Since the buffer is not accepting new cells, the buffer size either remains constant or decreases depending on the occurrence of a cell departure.

Finally, the matrix $\mathbf{D}_t$ describes the buffer's operation at the instant of buffer overflow when the buffer starts discarding cells. $\mathbf{D}_t$ has the form given in (5). Since the buffer is full at the point of overflow, the buffer size remains constant or it decreases. The matrices $\mathbf{D}_f$, $\mathbf{D}_e$, and $\mathbf{D}_t$ are used to specify the the entries of **C** for each slot.

We have tried to describe the system and the concept of the estimation algorithm as clearly as possible given the space limitation. A detailed description of the system and the estimation algorithm can be found in [1].

In summary, the slot number is defined using **P** and the arrival process for each slot is defined using **R**. The system behavior depends on the occurrence of cell arrivals. If there is a cell arrival ($\mathbf{C} = \mathbf{C}_a$) in the current slot, the possibility of buffer overflow will be indicated by the buffer occupancy that is preserved in $\mathbf{D}_{ij}$. If an overflow occurs, the system's next state and the time the system spends in that state is governed by the type of the current frame (i.e. the current slot number). The system transitions back to *accept* state after frame dependency (if any) terminates. The dropping algorithm is mainly implemented by the definition of **C** for each slot because it contains the state space the governs cell loss.

5 Simulation and Results

Segmented frames arrive to the first hop buffer where the order of frames (in repeating GOPs) is governed by the twelve-state machine that repeatedly produces an $IBBPBBPBBPBB$ pattern. This way the deterministic ordering between the frame types is preserved within each GOP to resemble better modeling accuracy than 3-state MMBP statistical ordering mentioned in [9]. Upon arrival, if space permits, segments are buffered in a FIFO fashion. If a frame segment overflows the buffer, that cell is discarded along with all successive cells that contain information dependent on that frame. Buffered segments are served at a constant rate.

[7] **D**(t,w,0,0) and **D**(t,w,0,2) cannot occur because the buffer neither accepts a cell nor overflows on no cell arrival.

$$\mathbf{D}_e = \begin{bmatrix} 1 & 0 & 0 & \cdots & 0 \\ \alpha & 1-\alpha & 0 & & \\ 0 & \alpha & 1-\alpha & & \vdots \\ \vdots & \ddots & \ddots & \ddots & 0 \\ 0 & \cdots & 0 & \alpha & 1-\alpha \end{bmatrix} \quad and \;\; \mathbf{D}_t = \begin{bmatrix} 0 & 0 & 0 & \cdots & 0 \\ 0 & 0 & 0 & \cdots & 0 \\ \vdots & \vdots & \vdots & & \vdots \\ 0 & 0 & 0 & \cdots & 0 \\ 0 & \cdots & 0 & \alpha & 1-\alpha \end{bmatrix} \tag{5}$$

In this work, frames are sized according to a lognormal distributions [6]. They are bounded by a maximum frame size. The mean size of each frame type is selected according to the average of statistics for real MPEG-2 coded movies shown in [4], which were prepared by Oliver Rose of the Computer Science Institute at University of Wuerzburg. The I-, P-, and B-frames are set to have normalized mean frame sizes, $\mu_I : \mu_P : \mu_B$, of $1 : 0.3 : 0.13$ and relative standard deviations, $\sigma_I : \sigma_P : \sigma_B$, of $1 : 0.76 : 0.32$, respectively. The ratios between different frame statistics reflect the correlation between frames in MPEG-2 video streams. The inter-GOP correlation, however, is not implemented in this traffic model since the variation in the total GOP size is greatly affected by scene changes. Scenes may last for a relatively long time, which minimizes the effect of a finite buffer in improving the system performance or absorbing traffic bursts at GOP or scene level. Maintaining the previously mentioned average frame size ratios limits the system's offered load[8] to 23% because, even when μ_I is maximal, $\mu_B = 0.13\mu_I$. Even though the maximum load is low, video streams are time sensitive, which cause the input arrival rate to reach the peak rate during a cell burst (frame). This arrival pattern can cause buffer overflow when the output link is congested.

The maximum load that we could reach in this system obviously shows how underutilized the input channel is when a single video stream is transmitted with peak cell rate. This highlights the need to aggregate multiple VBR video flows in the same channel to increase the bandwidth utilization, which we will investigate in future work.

The presented analysis from Section 4 was used to estimate the frame goodput of the system. Individual steady state probability vectors for each slot were produced using LU decomposition techniques. The analysis was compared to a discrete event simulation of the system. As previously mentioned, goodput is defined as the ratio of the cells belonging to correctly displayable frames that are transmitted by the server on the system's output link to the total number of cells . Furthermore, we define $P_{loss} = 1 - goodput$; we choose these definitions of goodput and loss probability because they are more representative measures of the integrity of the end user's video quality than other measures [10].

[8] Offered load = (full slots/Total slots) at the input link.

We compared the results of our analysis with the corresponding simulation results. In Figures 3–4, we plotted cell loss probability versus normalized output line rate[9] for different buffer sizes and different loads. The data in Figure 3(a) shows the loss probability plotted for several buffer sizes that range from two to four times the maximum frame size; simulation and analysis results compare favorably for that range of buffer sizes. Notice that, for an applied load of 0.2 and a buffer size of 60 cells, a loss probability of 10^{-6} can only be achieved when the normalized output rate is 0.28[10], which is equal to 71% bandwidth utilization instead of 20% at the input line. This highlights the effect of buffer smoothing on bandwidth utilization and peak cell rate.

It is noticed in both Figures 3(a) and 3(b) that the simulation results get closer to those of the analysis as the buffer size or the losses increase. These results are intuitive and expected.

In Figure 4, the effect of load on loss probability estimation is illustrated. Our estimation algorithm works well for different system loads. As expected, when load is increased, cell loss increases as well; notice that the proposed estimation method works well in that given region of buffer sizes. As the load decreases, the error slightly increases due to a smaller number of cell arrivals (lower load) in the simulation that are taken into account in the calculation of the loss. The estimation method works very well in that region and for relatively large buffer sizes as well and it matches the simulation results very closely.

6 Conclusions and Future Work

The goodput of a buffer with a video traffic input source was investigated. An approximate method was proposed to estimate the buffer behavior under highly correlated traffic sources and this method was verified using simulation. The simulation results and the estimation analysis results closely agree over a wide range of buffer sizes and load bounds. It is noted that a buffer that is three times the maximum frame size is sufficient to give a loss probability of 10^{-6} for

[9] The normalized output rate is the ratio between the output line rate and the input line rate. It can be looked at as a measure of link congestion.

[10] The relationship between load and output line rate is a function of the MPEG stream burstiness. Studying this relationship is outside the scope of this paper.

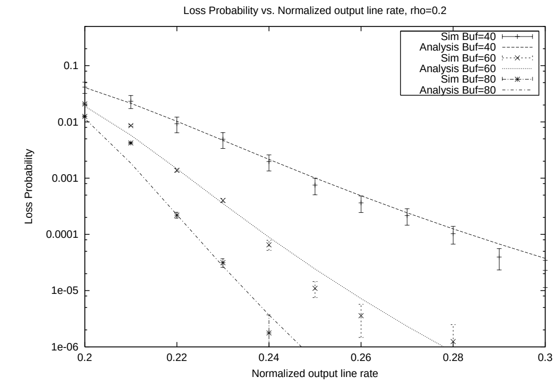

(a) “Lower” Utilization.

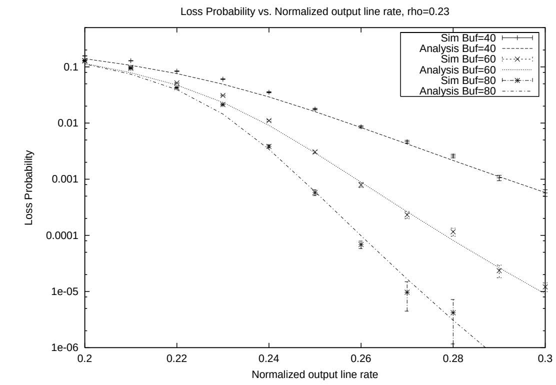

(b) “Higher” Utilization.

Figure 3. Loss Probabilities versus normalized output line rate.

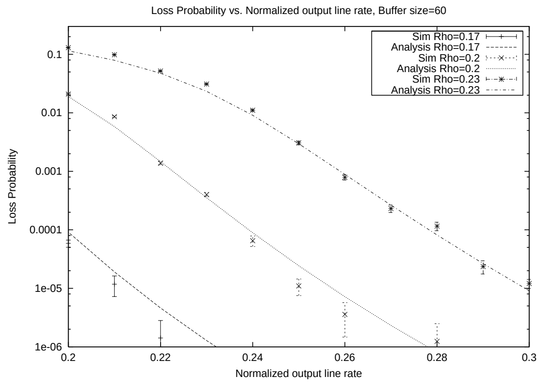

Figure 4. Effect of load on loss probability.

a load of 20% at a normalized output line rate of 0.28. This system situation can be viewed as a multiplexed system that provides each source with a normalized service rate of 0.28 and an allocated buffer size of three frame sizes. We also showed the effect of varying the output-to-input line rate ratio on the loss probability, which gives an indication of what maximum number of sources (output line speed drop) will still result in acceptable performance. This estimate can be applied to many switching systems near access networks for congestion control and rate allocation.

The next step in this work is to enhance the cell discard algorithm to include priority assignments to frames, which is expected to increase the system frame goodput to a level that makes it comparable to the conventional cell loss computation under the same network conditions.

References

[1] A. Awad, M. W. McKinnon, and R. Sivakumar. Goodput Analysis of Network Access Node Priority Buffers Carrying MPEG-2 Video Source. *Unpublished Manuscript, http://www.cnd.gatech.edu/˜ashraf/publications/Report.ps*, 2002.

[2] Z. Cao, Z. Wang, and E. Zegura. Rainbow Fair Queueing: Fair Bandwidth Sharing Without Per-Flow State. *Annual Joint Conference of the IEEE Computer and Communications Societies*, 2:922–31, March 2000.

[3] I. Feng, K.-T. Lo, H. Mehrpour, and A. Karbowiak. Cell Loss Concealment Method for MPEG Video in ATM Networks. *IEEE Global Telecomm. Conference.*, 3:1925–9, Nov. 1995.

[4] M. Frey and S. Nguyen-Quang. A Gamma-Based Framework for Modeling Variable MPEG Video Sources: The GOP GBAR Model. *IEEE/ACM ToN*, 8(6):710–9, December 2000.

[5] M. Krunz and H. Hughes. A Performance Study of Loss Probability for MPEG Video Traffic. *IEEE International Conference on Communications*, 3:1756–60, 1995.

[6] M. Krunz, R. Sass, and H. Hughes. Statistical Characteristics and Multiplexing of MPEG Streams. *INFOCOM'95*, 2:455–62, April 1995.

[7] J. R. Li, X. Gao, L. Qian, and V. Bharghavan. Goodput Control for Heterogeneous Data Streams. *NOSSDAV*, June 2000.

[8] J. L. Mitchell. *MPEG Video Compression Standard*. Digital multimemdia standards series. New York:Chapman & Hall, 1997.

[9] C. Ohta, K. Shinagawa, and Y. Onozato. Cell Loss Properties for Multiplexing of MPEG Video Sources Considering Picture Coding Types in ATM Networks. *ICC*, 3:23–7, June 1996.

[10] O. Verscheure, P. Frossard, and M. Hamdi. Joint Impact of MPEG-2 Encoding Rate and ATM Cell Losses on Video Quality. *GLOBECOM '98*, 1:71–6, Nov. 1998.

[11] D. Wilson and M. Ghanbari. An Efficient Loss Priority Scheme for MPEG-2 Variable Bit Rate Video for ATM Networks. *Global Telecommunications Conference.*, 3:1954–58, Nov. 1996.

[12] L. Zhang, D. Chow, and C. Hock Ng. Cell Loss Effect on QoS for MPEG Video Transmission in ATM Networks. *IEEE ICC*, 1:147–51, June 1999.